ELSEVIER

Quaternary Science Reviews 23 (2004) 1873–1878

QSR
RAPID COMMUNICATION

Rapid Communication

Does interplanetary dust control 100 kyr glacial cycles?

Gisela Winckler[a,*], Robert F. Anderson[a,b], Martin Stute[a,b,c], Peter Schlosser[a,b,d]

[a]*Lamont–Doherty Earth Observatory, Columbia University, 61 Route 9W, Palisades, NY 10964, USA*
[b]*Department of Earth & Environmental Sciences, Columbia University, New York, NY 10027, USA*
[c]*Department of Environmental Science, Barnard College, 3009 Broadway, New York, NY 10027, USA*
[d]*Department of Earth & Environmental Engineering, Columbia University, 500 W 120th St, New York, NY 10027, USA*

Received 22 October 2003; accepted 25 May 2004

Abstract

The cause of the 100 kyr glacial–interglacial cycles during the past 800 kyr is one of the fundamental puzzles in paleoclimatology. The widely accepted Milankovitch theory, relating earth's climate cycles to variations in insolation caused by periodic changes in orbital parameters, has difficulties to explain the predominant 100 kyr rhythm. Although earth's eccentricity varies with a period of 100 kyr, the resulting change in insolation is too small to produce the corresponding climate cycle by direct forcing (Imbrie et al., Paleoceanography 8 (1993) 699). In order to solve the '100 kyr problem', Muller and MacDonald (Nature 377 (1995) 107; Science 277 (1997a) 215; Proc. Nat. Acad. Sci. USA 94 (1997b) 8329) proposed an alternative orbital but non-Milankovitch mechanism attributing the glacial cycles to regular variations in the accretion of interplanetary dust particles (IDP) caused by 100 kyr cycles in the orbital inclination of the earth. To test this controversial hypothesis, we study the IDP accumulation in deep-sea sediments from a period in the early Pleistocene. We find apparent 41 kyr cycles but no 100 kyr periodicity in the IDP accumulation rate. As there is no known mechanism to produce 41 kyr cycles in IDP supply from space, we conclude that the 41 kyr cycles are caused by the dynamics of sediment accumulation, and that changes in the IDP flux do not drive the Pleistocene glacial cycles.

1. Introduction

According to the inclination hypothesis, the oscillations of the orbital inclination cause the earth to periodically pass through a cloud of IDPs. The key link between variable IDP accretion and climate is believed to involve noctilucent clouds. As IDPs provide nucleation sites for noctilucent clouds, the accretion rate of IDPs is suggested to influence the cloud opacity and, in turn, affect the earth's climate (Muller and MacDonald, 1997b).

Two major pieces of evidence support the inclination hypothesis. First, spectral analysis of $\delta^{18}O$ in foraminiferal $CaCO_3$, a proxy of global ice volume, shows a single narrow peak at a period of 100 kyr. This matches the single 100 kyr peak expected from inclination variations, whereas it is in disagreement with the triplet peak (two distinct peaks at 95 and 124 kyr, one at 404 kyr) expected from eccentricity (Berger and Loutre, 1992). A number of models have been developed to address the incompatibility between the single narrow peak observed in $\delta^{18}O$ records and the pattern expected from eccentricity. These invoke, for example, frequency modulation (Rial, 1999), suppression of the two longer eccentricity periods (Berger, 1999), and trigger mechanisms (Ridgwell et al., 1999); however, the implications of these modeling approaches remain controversial.

Second, the inclination hypothesis predicts periodic changes in the accretion of IDPs. Using extraterrestrial ^3He as a proxy of interplanetary dust[1] (e.g., Farley, 2001), such regular 100 kyr cycles have been identified in

*Corresponding author: Tel.: +1-845-365-8756; fax: +1-845-365-8155.
E-mail address: winckler@ldeo.columbia.edu (G. Winckler).

[1]IDPs derive their helium isotope signal from implantation of solar wind ions. They are highly enriched in helium, particularly in ^3He, compared to terrigeneous matter and can be readily detected in most marine sediment environments.

0277-3791/$ - see front matter © 2004 Elsevier Ltd. All rights reserved.
doi:10.1016/j.quascirev.2004.05.007

late Pleistocene sediments at various locations, including the North Atlantic at Ocean Drilling Program (ODP) site 607 (Farley and Patterson, 1995), the Ontong Java Plateau at ODP site 806 (Patterson and Farley, 1998) and the eastern equatorial Pacific (Marcantonio et al., 1995, 1996). However, there has been considerable debate whether the 100 kyr cycles in ^{3}He accumulation rate reflect the variability of IDP accretion to earth or rather climate-related changes in sediment redistribution (Marcantonio et al., 1996, 2001; Higgins et al., 2002). Resolution of this issue has been hampered by the limitation that all ^{3}He studies to date have focused on the late Pleistocene when both the inclination and earth's climate display a dominant 100 kyr period of variability.

Here, we present a new approach to test the inclination hypothesis by studying the ^{3}He accretion in the early Pleistocene ('the 41 kyr world'), when global ice volume varied almost exclusively at the 41 kyr obliquity period (Fig. 1B) while inclination of the earth's orbit still displayed a 100 kyr periodicity (Fig. 1A). If 100 kyr cycles in ^{3}He accumulation existed in the '41 kyr world', Muller's view (Muller and MacDonald, 1995, 1997a, 1997b, 2000) that the flux of IDPs to earth varies with the inclination would be strongly supported. On the other hand, 41 kyr cycles in ^{3}He accumulation rates would support the view (Marcantonio et al., 1996; Higgins et al., 2002) that Pleistocene cycles of IDP accumulation are caused by factors unrelated to changes in the supply of IDPs from space.

2. Methods

The sediments studied are from ODP site 849 (Leg 138) in the eastern equatorial Pacific (110 W, 0.1 N, 3700 m water depth). The age model (time period 0.6–2.5 Ma) for ODP site 849, provided by Mix et al. (1995), was developed by correlating the δ^{18}O record of ODP site 849 to the δ^{18}O record from ODP site 677, using the timescale of Shackleton et al. (1990).

Sample details and helium isotope data from ODP849 are given in Table 1.

Extraterrestrial helium was measured at high resolution (approximately 4 kyr) on samples taken between 39 and 44.6 rmcd (revised meters composite depth), an interval that represents $\sim$240 kyr between 1.36 and 1.6 Ma. Samples were selected corresponding to the depths of the original δ^{18}O study (Mix et al., 1995) and span 6 obliquity (41 kyr) cycles. Samples of 0.75–1.5 g were leached with 0.5 N acetic acid to remove the calcium carbonate. The helium was extracted from the non-carbonate fraction of the samples at about 1300 °C and measured on a MAP-215 mass spectrometer (Marcantonio et al., 1995). While the typical analytical error of the mass spectrometric analysis is 1–3% (Table 1), the actual uncertainty of the ^{3}He measurement is controlled by the statistical effect of the small number of IDPs hosted in the sediments. To account for this effect, 18 of the measurements were replicated. The reproducibility distribution of these replicates is in good agreement with the model prediction (Farley et al., 1997) and, therefore, the distribution can be approximated by a Gaussian distribution with 1σ uncertainty of 20% (Patterson and Farley, 1998). The ^{3}He/^{4}He ratios range from 7×10^{-5} to 2×10^{-4} compared to $1\text{–}4\times10^{-4}$ in pure IDP (Nier and Schlutter, 1992) and $2\text{–}4\times10^{-8}$ in terrigeneous material (Mamyrin and Tolstikhin, 1984) implying that virtually all of the ^{3}He is of extraterrestrial origin.

3. Results and discussion

The obliquity cycle is clearly evident in the δ^{18}O record (Fig. 1B), in the $CaCO_3$ content of the sediments (Fig. 1C) and the extraterrestrial ^{3}He concentrations (Fig. 1D). The ^{3}He accumulation rates (Fig. 1F) were derived by multiplying the ^{3}He concentrations with the ^{18}O derived bulk mass accumulation rates (Fig. 1E). They show a cyclic variation that is to a large degree coherent with the δ^{18}O signal with the exception of the penultimate maximum at 1.437 Ma, which appears to be slightly shifted relative to the respective δ^{18}O peak.

Averaging the ^{3}He accumulation rate over the length of the record and comparing it to fluxes reported for the late Pleistocene allows us to evaluate long-term changes in the extraterrestrial ^{3}He accretion to earth. The mean ^{3}He accumulation rate obtained for the early Pleistocene is $7.3\pm1.8\times10^{-13}$ cm^3 cm^{-2} kyr^{-1} and is indistinguishable from the estimates for the mean flux of the past 200 kyr ($8.0\pm2.4\times10^{-13}$ cm^3 cm^{-2} kyr^{-1}, Marcantonio et al., 2001) and the flux determined from ice core studies ($6.2\pm2.7\times10^{-13}$ cm^3 cm^{-2} kyr^{-1} for Greenland/GISP2 and $7.7\pm2.5\times10^{-13}$ cm^3 cm^{-2} kyr^{-1} for Antarctica/Vostok, Brook et al., 2000). The agreement implies that there is no sudden increase in interplanetary dust levels between the early Pleistocene and the late Pleistocene as has been suggested earlier (Farley, 1995; Muller and MacDonald, 2000).

In order to characterize in greater detail the systematic variations of the ^{3}He accumulation rates, a spectral analysis of the δ^{18}O (Fig. 2A) and ^{3}He accumulation rates (Fig. 2B) was performed using the maximum entropy method. Strongest power in both spectra is observed at ca. 0.024 cycles kyr^{-1}, corresponding to the periodicity of obliquity (41 kyr) and confirming what is visually seen in Fig. 1E. No other peaks significant at the 95% level are detected. We recognize that the record spans only about 2.5 inclination cycles (100 kyr period) possibly affecting the spectral definition at such low frequencies and that longer records, as they become

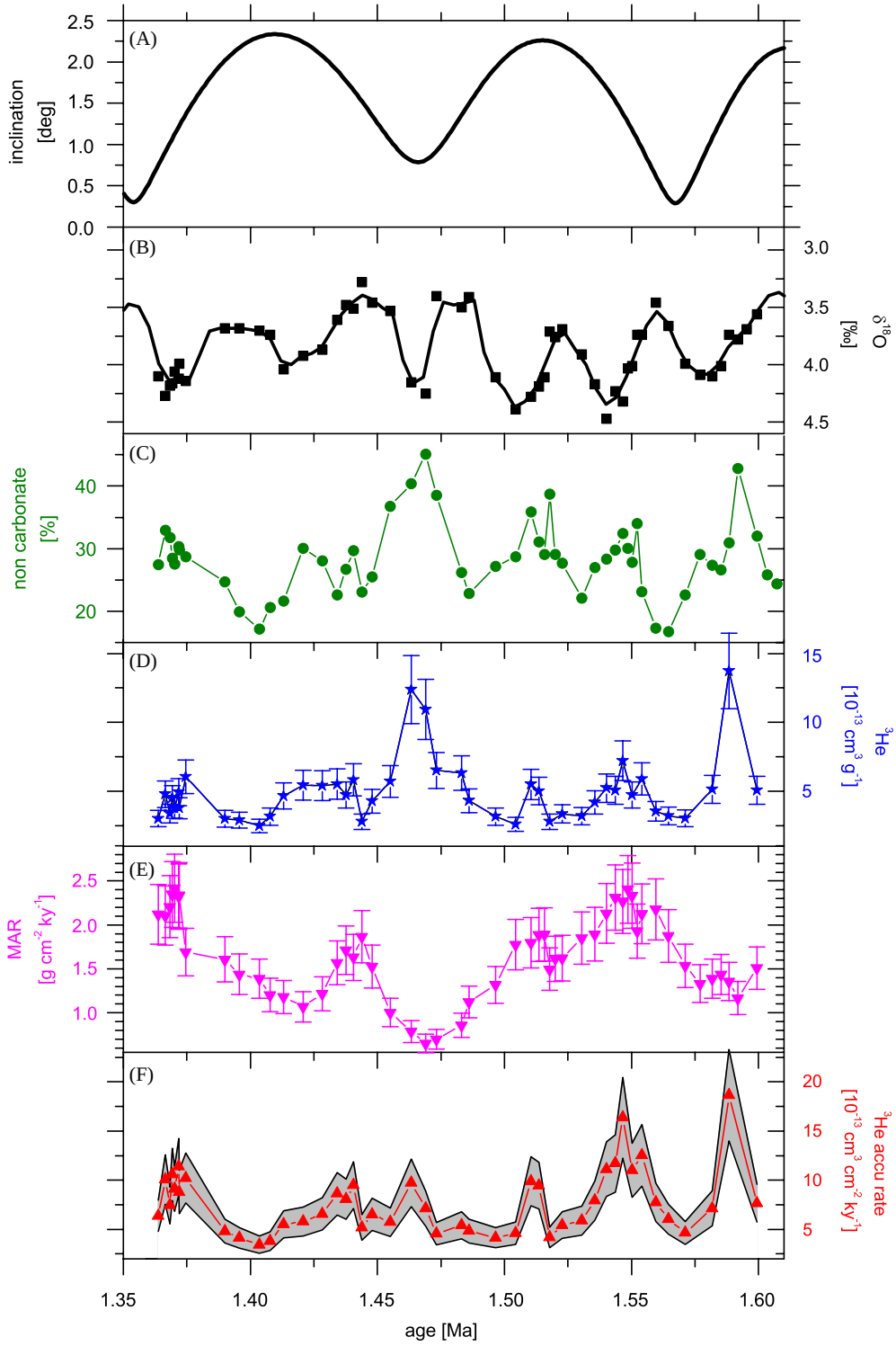

Fig. 1. Inclination and down-core profiles for core ODP849, plotted against $\delta^{18}O$ based age, for the time-slice between 1.35 and 1.61 Ma. (A) Inclination of the earth's orbit relative to the invariable plane (http://www-muller.lbl.gov). (B) $\delta^{18}O$ of benthic foraminifera (Mix et al., 1995). (C) Calcium carbonate content given as non-carbonate content [100-$CaCO_3$%] to align the peaks. (D) Extraterrestrial ^{3}He concentration. (E) $\delta^{18}O$-derived mass accumulation rates. (F) Extraterrestrial ^{3}He accumulation rate; ^{3}He accumulation rates are derived by multiplying the ^{3}He concentration with the $\delta^{18}O$-derived mass accumulation rates. The amplitude peak-to-trough of the ^{3}He accumulation rates is about a factor of 2–4, significantly larger than the uncertainty, indicated by the gray envelope. The 1σ uncertainty includes the uncertainty of the ^{3}He concentration (20%) and the uncertainty of the bulk mass accumulation rates (16%).

Table 1
ODP 849: sample details and helium isotope data

Section	Depth (cm)	Depth (rmcd)	Age[a] (Ma)	$\delta^{18}O$[a] (‰)	^3He[b] (10^{-13} cm^3 g^{-1})	$^3He/^4He$[b] (R/R_a)	$CaCO_3$[c] (%)	MAR[d] (g cm^{-2} kyr^{-1})
849C-4H-3[e]	16	38.98	1.364	4.10	3.007 ± 0.058	88.6 ± 1.2	72.6	2.12
849C-4H-3	26	39.08	1.367	4.27	4.784 ± 0.097	93.4 ± 1.4	67.1	2.11
849D-4H-1	16	39.15	1.368	4.18	3.369 ± 0.095	104.5 ± 2.6	68.2	2.21
849C-4H-3[e]	36	39.18	1.369	4.16	4.514 ± 0.153	55.6 ± 1.6	71.5	2.35
849D-4H-1	26	39.22	1.370	4.06	3.769 ± 0.090	106.4 ± 2.0	72.5	2.42
849C-4H-3	46	39.28	1.372	4.12	4.914 ± 0.192	82.9 ± 3.0	69.7	2.32
849D-4H-1	36	39.29	1.372	3.99	3.766 ± 0.087	92.0 ± 1.6	70.2	2.34
849D-4H-1	46	39.39	1.375	4.14	6.053 ± 0.097	50.5 ± 0.4	71.3	1.69
849D-4H-1[e]	66	39.78	1.390	3.68	3.001 ± 0.060	125.6 ± 1.3	75.3	1.61
849D-4H-1	76	39.9	1.396	3.68	2.885 ± 0.077	131.6 ± 2.5	80.1	1.44
849D-4H-1	96	40.05	1.404	3.70	2.482 ± 0.066	105.9 ± 2.4	82.8	1.39
849D-4H-1	106	40.12	1.408	3.74	3.156 ± 0.057	106.6 ± 1.0	79.4	1.20
849D-4H-1	116	40.21	1.413	4.04	4.657 ± 0.100	100 ± 1.6	78.4	1.18
849D-4H-1[e]	126	40.34	1.421	3.92	5.428 ± 0.071	93.5 ± 0.8	70.0	1.07
849D-4H-1	136	40.48	1.428	3.87	5.398 ± 0.100	103.0 ± 0.9	72.0	1.22
849D-4H-1[e]	146	40.6	1.434	3.61	5.505 ± 0.084	137.6 ± 1.3	77.4	1.57
849D-4H-2	6	40.69	1.438	3.48	4.714 ± 0.070	114.6 ± 1.2	73.3	1.71
849D-4H-2[e]	16	40.77	1.441	3.51	5.814 ± 0.107	117.5 ± 1.5	70.3	1.63
849D-4H-2[e]	26	40.86	1.444	3.28	2.781 ± 0.066	82.9 ± 1.5	76.9	1.87
849D-4H-2	36	40.97	1.448	3.46	4.268 ± 0.082	88.9 ± 1.2	74.5	1.53
849D-4H-2[e]	46	41.12	1.455	3.53	5.709 ± 0.088	59.5 ± 0.9	63.2	1.00
849D-4H-2[e]	56	41.26	1.463	4.15	12.368 ± 0.169	98.7 ± 1.0	59.6	0.79
849D-4H-2[e]	66	41.34	1.469	4.25	10.927 ± 0.124	91.9 ± 0.7	54.9	0.65
849D-4H-2	76	41.4	1.473	3.40	6.503 ± 0.136	101.0 ± 1.3	61.4	0.70
849D-4H-2	106	41.53	1.483	3.5	6.320 ± 0.140	93.0 ± 1.7	73.8	0.86
849D-4H-2	116	41.57	1.486	3.41	4.306 ± 0.097	137.0 ± 2.2	77.2	1.12
849D-4H-2	136	41.75	1.497	4.11	3.156 ± 0.069	6.6 ± 0.1	72.9	1.32
849D-4H-2	146	41.95	1.504	4.39	2.590 ± 0.095	81.9 ± 2.6	71.3	1.78
849D-4H-3[e]	6	42.15	1.510	4.28	5.500 ± 0.083	93.4 ± 1.0	64.1	1.80
849D-4H-3[e]	16	42.25	1.514	4.19	5.005 ± 0.091	103.6 ± 1.4	68.9	1.89
849D-4H-3[e]	36	42.38	1.518	3.71	2.790 ± 0.075	110.8 ± 2.0	61.3	1.50
849D-4H-3[e]	56	42.51	1.523	3.69	3.349 ± 0.084	104.5 ± 2.0	72.3	1.62
849D-4H-3	76	42.71	1.530	3.91	3.184 ± 0.072	67.2 ± 1.1	77.9	1.85
849D-4H-3	86	42.85	1.535	4.17	4.190 ± 0.085	75.5 ± 1.2	73.0	1.89
849D-4H-3	96	43.00	1.540	4.47	5.218 ± 0.163	81.8 ± 2.4	71.6	2.13
849D-4H-3	106	43.13	1.544	4.23	5.063 ± 0.107	87.4 ± 1.4	70.3	2.31
849D-4H-3	116	43.24	1.546	4.32	7.211 ± 0.166	101.0 ± 1.8	67.6	2.27
849D-4H-3[e]	136	43.39	1.550	4.01	4.724 ± 0.070	71.8 ± 1.0	72.2	2.33
849D-4H-4[e]	6	43.52	1.554	3.74	5.888 ± 0.125	57.3 ± 1.1	76.9	2.13
849D-4H-4	26	43.69	1.560	3.46	3.551 ± 0.098	129.1 ± 2.8	82.7	2.18
849D-4H-4	36	43.82	1.564	3.66	3.210 ± 0.044	121.6 ± 1.0	83.3	1.88
849D-4H-4	46	43.97	1.571	3.99	3.022 ± 0.049	98.6 ± 1.0	77.4	1.54
849D-4H-4	66	44.2	1.582	4.10	5.132 ± 0.138	113.1 ± 2.7	72.7	1.39
849D-4H-4[e]	86	44.35	1.588	3.74	13.742 ± 0.192	126.6 ± 1.0	69.0	1.36
849D-4H-4[e]	116	44.62	1.599	3.56	5.074 ± 0.090	109.2 ± 1.3	68.0	1.51

[a]Age model and $\delta^{18}O$ data are from Mix et al. (1995).

[b]^3He concentrations are reported in units of cm^3 STP per gram of sediment, $^3He/^4He$ ratios are normalized to the atmospheric $^3He/^4He$ ratio ($R_a = 1.384 \times 10^{-6}$). Errors are the analytical uncertainties of the mass spectrometric analysis.

[c]$CaCO_3$ contents were measured by standard coulometric procedures at L-DEO.

[d]Bulk mass accumulation rates (MAR) were calculated by multiplying the linear sedimentation rate (LSR) from the oxygen isotope stratigraphy by Mix et al. (1995) by the dry bulk density (DBD). A LSR was assigned to each sample as $LSR = [depth(n+1) - depth(n-1)]/[age(n+1) - age(n-1)]$. DBD were derived from the $CaCO_3$ content data by using the empirical relationship for equatorial Pacific carbonate sediments developed by Murray and Leinen (1993).

[e]Marked samples were replicated for helium isotope analysis. In these cases, average values of replicates are reported.

available, will be essential to improve confidence levels for the low end of the spectrum. However, as is apparent from Figs. 1F and 2B, the spectral power in the ^3He accumulation record is clearly dominated by the 41 kyr obliquity cycle while any lower frequencies are at most of secondary importance. In particular, the spectral

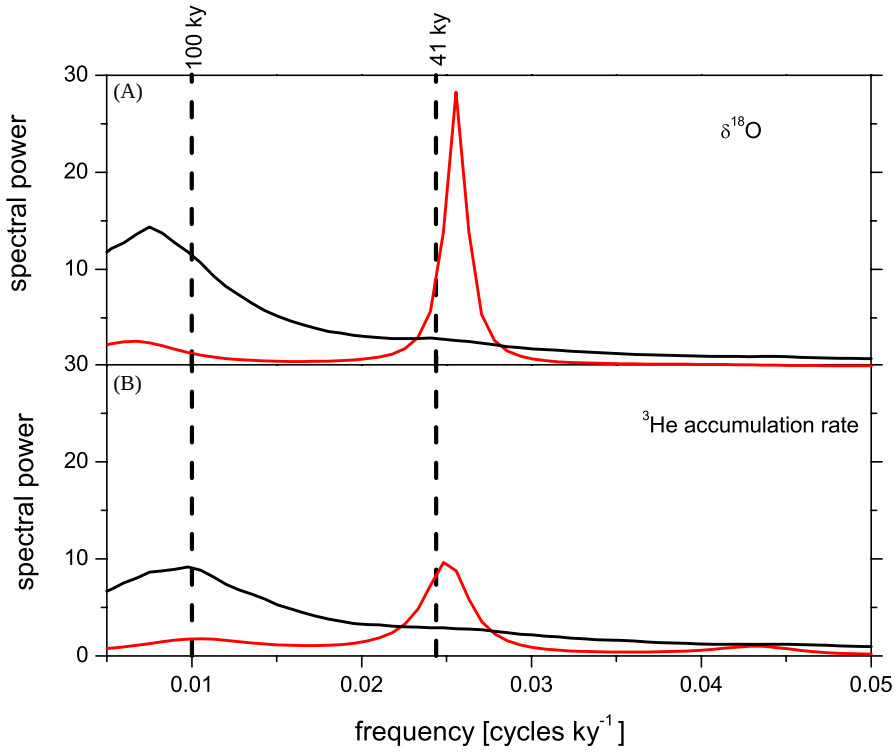

Fig. 2. Spectral power (red line) of $\delta^{18}O$ (A) and ^{3}He accumulation rates (B) were calculated using maximum entropy spectrum analysis. The data were interpolated to evenly spaced points (5 kyr), the order of the autoregressive process was 10. The 95% significance level (black line) was calculated from Monte Carlo simulations (5000 runs) of red noise (autoregressive process of order 1) fitted to the data.

analysis of the ^{3}He accumulation record does not support a signal at the frequency of the earth's inclination (0.01 cycles kyr^{-1} = 100 kyr).

Consequently, as there is no plausible mechanism to produce 41 kyr variability in the supply of IDPs to earth, we conclude that the periodicity seen in the ^{3}He accumulation rate does not reflect cyclical changes in the source of IDPs but rather, as reflected in the strong spectral power at 41 kyr, it derives from climate-related processes that influence the inferred sediment accumulation rates. Maxima of the ^{3}He accumulation (Fig. 1F) correspond to periods of continental ice sheet growth (i.e., increasing $\delta^{18}O$), or to peak glacial conditions (max $\delta^{18}O$, Fig. 1B) as well as to minima in the $CaCO_3$ content (Fig. 1C). This relationship is consistent with that observed in late Pleistocene records in the equatorial Pacific Ocean (e.g., Marcantonio et al., 1996). In addition, the amplitude of the oscillations in the 41 kyr world is comparable to the amplitude observed in the late Pleistocene. These similarities imply a common mechanism driving the apparent variability in ^{3}He accumulation rate throughout the Pleistocene.

4. Conclusions

The lack of significant power at 0.01 cycles kyr^{-1} in the accumulation rate of ^{3}He strongly suggests that there is no 100 kyr periodicity in the accretion rate of IDPs in the early Pleistocene. This indicates that changes in the inclination of earth's orbit do not alter measurably the supply of IDPs from space. Being a necessary condition for the inclination hypothesis, this absence leads us to conclude that inclination-related changes in the accretion of interplanetary dust are not the driver of late Pleistocene glacial cycles. Our finding that apparent cycles of IDP accumulation during the early Pleistocene (41 kyr cycles) bear a relationship to global ice volume and to the $CaCO_3$ content of sediments similar to that seen in the late Pleistocene (100 kyr cycles) supports this conclusion.

Whether the apparent ^{3}He accumulation cycles result from climate-related changes in sediment redistribution (e.g., Marcantonio et al., 1996, 2001; Higgins et al., 2002), or from systematic inaccuracies of the $\delta^{18}O$-derived age model potentially introduced by carbonate dissolution, the accumulation rates of other sedimentary constituents will be affected similarly. Paleoceanographic studies that rely on such accumulation rates must take this into account to prevent misinterpretations of deep-sea sediment fluxes. Future work, including studies of independent proxies of sediment redistribution (e.g., grain size analysis), and modeling will allow us to determine the exact nature of the patterns observed.

Acknowledgements

This research used samples provided by the Ocean Drilling Program (ODP). ODP is sponsored by the US National Science Foundation (NSF) and participating countries under management of Joint Oceanographic Institutions (JOI), Inc. Funding for this research was provided by NSF grant OCE0221333. We thank R. Muller and E. Brook for constructive reviews. G.W. wishes to thank the Comer Science & Education Foundation for support, and Joerg Schaefer and Hubertus Fischer for fruitful discussions. This is L-DEO contribution #6623.

References

Berger, W.H., 1999. The 100-kyr ice-age cycle: internal oscillation or inclinational forcing. International Journal of Earth Science 88, 305–316.

Berger, A., Loutre, M.F., 1992. Astronomical solutions for paleoclimate studies over the last 3 million years. Earth and Planetary Science Letters 111, 369–382.

Brook, E.J., Kurz, M.D., Curtice, J., Cowburn, S., 2000. Accretion of interplanetary dust in polar ice. Geophysical Research Letters 27, 3145–3148.

Farley, K.A., 1995. Cenozoic variations in the flux of interplanetary dust recorded by ^{3}He in a deep-sea sediment. Nature 376, 153–156.

Farley, K.A., 2001. Extraterrestrial helium in seafloor sediments: identification, characteristics, and accretion rate over geological time. In: Peucker-Ehrenbrink, B., Schmitz, B. (Eds.), Accretion of Extraterrestrial Matter Throughout Earth's History. Kluwer Academic/Plenum Publishers, New York, pp. 179–204.

Farley, K.A., Patterson, D.B., 1995. A 100-kyr periodicity in the flux of extraterrestrial ^{3}He to the sea floor. Nature 378, 600–603.

Farley, K.A., Love, S.G., Patterson, D.B., 1997. Atmospheric entry heating and helium retentivity of interplanetary dust particles. Geochimica et Cosmochimica Acta 61, 2309–2316.

Higgins, S.M., Anderson, R.F., Marcantonio, F., Schlosser, M., Stute, M., 2002. Sediment focusing creates 100-ka cycles in interplanetary dust accumulation on the Ontong Java Plateau. Earth and Planetary Science Letters 203, 383–397.

Imbrie, J., Berger, A., Boyle, E., Clemens, S., Duffy, A., Howard, W., Kukla, G., Kutzbach, J., Martinson, D., McIntyre, A., Mix, A., Molfino, B., Morley, J., Peterson, J., Pisias, N., Prell, W., Raymo, M., Shackleton, N., 1993. On the structure and origin of major glaciation cycles 2: the 100,000 year cycle. Paleoceanography 8, 699–735.

Mamyrin, B.A., Tolstikhin, I.N., 1984. Helium Isotopes in Nature. Elsevier, Amsterdam, 273pp.

Marcantonio, F., Kumar, N., Stute, M., Anderson, R.F., Seidl, M.A., Schlosser, P., Mix, A., 1995. A comparative study of accumulation rates derived by He and Th isotope analysis of marine sediments. Earth and Planetary Science Letters 133, 549–555.

Marcantonio, F., Anderson, R.F., Stute, M., Kumar, N., Schlosser, P., Mix, A., 1996. Extraterrestrial ^{3}He as a tracer of marine sediment transport and accumulation. Nature 383, 705–707.

Marcantonio, F., Anderson, R.F., Higgins, S., Stute, M., Schlosser, P., Kubik, P., 2001. Sediment focusing in the central equatorial Pacific Ocean. Paleoceanography 16, 260–267.

Mix, A.C., Pisias, N.G., Rugh, W., Wilson, J., Morey, A., Hagelberg, T.K., 1995. Benthic foraminifer stable isotope record from Site 849 (0–5 Ma): local and global climate changes. In: Pisias, N.G., Mayer, L.A., Janecek, T.R., Palmer-Julson, A., van Andel, T.H. (Eds.), Proceedings of the Ocean Drilling Program, Scientific Results. Ocean Drilling Program, College Station, Tx, pp. 371–412.

Muller, R.A., MacDonald, G.J., 1995. Glacial cycles and orbital inclination. Nature 377, 107–108.

Muller, R.A., MacDonald, G.J., 1997a. Glacial cycling and astronomical forcing. Science 277, 215–218.

Muller, R.A., MacDonald, G.J., 1997b. Spectrum of 100 kyr glacial cycle: orbital inclination, not eccentricity. Proceedings of the National Academy of Science USA 94, 8329–8334.

Muller, R.A., MacDonald, G.J., 2000. Ice ages and astronomical causes. Data, Spectral Analysis, Mechanisms. Springer Praxis, Chichester, 318pp.

Murray, R.W., Leinen, M., 1993. Chemical transport to the seafloor of the equatorial Pacific Ocean across a latitudinal transect at 135 W: tracking sedimentary major, trace, and rare earth element fluxes at the Equator and the Intertropical Convergence Zone. Geochimica et Cosmochimica Acta 57, 4141–4163.

Nier, A.O., Schlutter, D.J., 1992. Extraction of helium from individual interplanetary dust particles by step-heating. Meteoritics 27, 166–173.

Patterson, D.B., Farley, K.A., 1998. Extraterrestrial ^{3}He in seafloor sediments: evidence for correlated 100 kyr periodicity in the accretion rate of interplanetary dust, orbital parameters, and Quarternary climate. Geochimica et Cosmochimica Acta 62, 3669–3682.

Rial, J.A., 1999. Pacemaking the ice ages by frequency modulation of earth's orbital eccentricity. Science 285, 564–568.

Ridgwell, A.J., Watson, A.J., Raymo, M.E., 1999. Is the spectral signature of the 100 kyr glacial cycle consistent with a Milankovitch origin? Paleoceanography 14, 437–440.

Shackleton, N., Berger, A., Peltier, W.R., 1990. An alternative astronomical calibration of the lower Pleistocene timescale based on ODP Site 677. Transactions of the Royal Society of Edinburgh—Earth Sciences 81, 251–261.